LA-UR- 11-00219

Approved for public release; distribution is unlimited.

Title:	A framework for developing a mimetic tensor artificial viscosity for Lagrangian hydrocodes on arbitrary polygonal and polyhedral meshes (U)
Author(s):	Konstantin Lipnikov & Mikhail Shashkov
Intended for:	Proceedings for the MECDC 2010 Conference

Los Alamos
NATIONAL LABORATORY
EST. 1943

Form 836 (7/06)

LAUR 10-00043

UNCLASSIFIED

August 30, 2010

A framework for developing a mimetic tensor artificial viscosity for Lagrangian hydrocodes on arbitrary polygonal and polyhedral meshes (U)

[1]Konstantin Lipnikov, [1]Mikhail Shashkov
[1]*Los Alamos National Laboratory*
Mail Stop B284
LANL, Los Alamos, New Mexico
87545, USA

We construct a new mimetic tensor artificial viscosity on general polygonal and polyhedral meshes. The tensor artificial viscosity is based on a mimetic discretization of coordinate invariant operators, divergence of a tensor and gradient of a vector. The focus of this paper is on the symmetric form, div $(\mu\,\varepsilon(\mathbf{u}))$, of the tensor artificial viscosity where $\varepsilon(\mathbf{u})$ is the symmetrized gradient of $\mathbf{u}$ and μ is a tensor. The mimetic discretizations of this operator is derived for the case of a full tensor coefficient μ that may reflect a shock direction. We demonstrate performance of the new viscosity for the Noh implosion, Sedov explosion and Saltzman piston problems in both Cartesian and axisymmetric coordinate systems.

Prepared for Proceedings of the NECDC 2010

UNCLASSIFIED

Introduction

Consider a system of hydrodynamic equations in Lagrangian coordinates describing motion of an ideal compressible gas:

$$\begin{aligned} \frac{1}{\rho}\frac{D\rho}{Dt} &= -\mathrm{div}\,\mathbf{u}, \\ \rho\frac{D\mathbf{u}}{Dt} &= -\nabla \mathrm{p}, \\ \rho\frac{D\varepsilon}{Dt} &= -\mathrm{p}\,\mathrm{div}\,\mathbf{u}, \end{aligned}$$

where ρ, p, $\mathbf{u}$ and ε are the gas density, pressure, velocity and internal energy, respectively, and D/Dt denotes the material derivative. These equations represent fundamental conservation laws for the mass, momentum, and energy. The system of three equations has four unknowns; therefore, it is closed by an equation of state.

Modeling of high-speed flows with shocks using a staggered discretization [3] requires introduction of an *artificial numerical viscosity* [4, 10, 9]. It stabilizes the simulation by spreading the shock across a few mesh elements. In 1-D, the classical Von Neumann-Richtmyer viscosity [4] with a linear term due to Landshoff [9] has a clearly defined continuum analog. In particular, the modified momentum equation has the following form:

$$\rho\frac{D\mathbf{u}}{Dt} = -\frac{\partial p}{\partial x} + \frac{\partial}{\partial x}\left(\mu_{12}\frac{\partial \mathbf{u}}{\partial x}\right), \qquad (1)$$

where the viscosity coefficient μ_{12} depend on the solution:

$$\mu_{12}(\mathbf{u}) = \mu_1 - \frac{\mu_2}{\rho}\frac{\partial \mathbf{u}}{\partial x}.$$

The parameters μ_1 and μ_2 control shock thickness. Analysis of continuum equations for a strong shock with thickness of six mesh cells [12] (in the mass coordinates) gives $\mu_1 = c_1(\gamma+1)\rho s\Delta x$ and $\mu_2 = c_2(\gamma+1)\rho^2(\Delta x)^2$ with positive constants c_1 and c_2 close to one. Here s is the sound speed and Δx is the mesh size.

In 2-D, the basic requirements for design of the artificial viscosity, as well as overview of existing methods, can be found in [5]. Here, we propose an artificial viscosity model that satisfies four requirements: it is disspative, Galilean invariant, and self-similar motion invariant. More precisely, an analog of the modified momentum equation (1) is

$$\rho\frac{D\mathbf{u}}{Dt} = -\nabla p + \mathrm{div}\ (\mu_{12}\,\varepsilon(\mathbf{u}))$$

with the viscosity coefficient

$$\mu_{12}(\mathbf{u}) = \mu_1 - \frac{\mu_2}{\rho}\,\varepsilon(\mathbf{u}).$$

Here $\varepsilon(\mathbf{u})$ denotes the symmetrized gradient, $\varepsilon(\mathbf{u}) = \frac{1}{2}(\nabla\mathbf{u} + (\nabla\mathbf{u})^T)$.

For a staggered discretization [3] considered here, the discrete velocities are defined at mesh nodes, while the discrete pressure, density, and internal energy are defined on mesh elements. Unstructured and disturted polygonal and polyhedral meshes are challenging for desining an accurate discretization of the artificial viscosity term. In this paper, we employ a novel discretization tenchnology developed in [1] for a scalar diffusion operator. This technology represents recent progress in development of mimetic discretization methods and is based on a discrete tensor calculus. Applied to the term

$$\mathbf{f}^{vis} = \mathrm{div}\,(\mu_{12}\,\varepsilon(\mathbf{u})), \qquad (2)$$

where μ_{12} is a full tensor, it results in a novel tensor artificial viscosity (TAV) method that extends the original TAV method [7] with a scalar μ_{12}. The tensorial coefficient μ_{12} provides a tool for building various artificial viscosity models. In this paper we consider only second-order tensors; however, the mathematical structure of equations allows us to use full fourth-order tensors in the future.

The new TAV framework can be applied to meshes with nonconvex and degenerate elements. Note

that the related TAV methods [7, 8] are limited to meshes with convex elements.

Method description

Consider a partition of the computation domain $\Omega \in \Re^d$ into polygonal ($d = 2$) or polyhedral ($d = 3$) elements E that may be non-convex or degenerate. Let $|E|$ denote the volume of E.

Consider a conventional staggered discretization, where the degrees of freedom for velocity $\mathbf{u}$ are defined at mesh points. Let $\mathbf{U}$ be the vector of all velocity degrees of freedom. In 3-D, the size of $\mathbf{U}$ is triple the number of mesh points. We also need the restriction of this vector to element E that we denote by $\mathbf{U}_E$. The size of $\mathbf{U}_E$ is triple the number of vertices of E. Similarly, $\mathbf{U}_{E,v}$ denotes the restriction of $\mathbf{U}_E$ to vertex v of E. This is a three-dimensional vector.

Multiplying both sides of (2) by a test function $\mathbf{v}$, integrating by parts, and using proper boundary conditions, yields

$$\int_\Omega \mathbf{f}^{vis} \cdot \mathbf{v} \, \mathrm{d}V = -\int_\Omega (\mu_{12}\, \varepsilon(\mathbf{u})) : \varepsilon(\mathbf{v}) \, \mathrm{d}V.$$

We apply accurate (will be speficied later) quadrature rules to both integrals. Each quadrature rule is written as a vector-matrix-vector multiplication with vectors of degrees of freedom and a matrix of weights:

$$(\mathbf{F}^{vis})^T \, \mathbf{M} \, \mathbf{V} + \mathcal{O}(h) = -\mathbf{U}^T \, \mathbf{A} \, \mathbf{V} + \mathcal{O}(h),$$

where the $\mathbf{F}^{vis}$ is the global vector of point-based degrees of freedom of the force function $\mathbf{f}^{vis}$. The vector $\mathbf{V}$ is from the same discrete space as $\mathbf{U}$. The $\mathcal{O}(h)$ terms must be small for sufficiently smooth functions. Omitting these terms, we obtain the desired viscous forces at mesh points:

$$\mathbf{F}^{vis} = -\mathbf{M}^{-1} \mathbf{A} \, \mathbf{U}.$$

Note that the actual computations require only the vector $\mathbf{M}\,\mathbf{F}^{vis}$. Thus, our main focus is on the stiffness matrix $\mathbf{A}$. We assume that this matrix can be assembled from elemental matrices $\mathbf{A}_E$:

$$\mathbf{A} = \sum_{E \in \mathcal{T}_h} \mathbf{N}_E \mathbf{A}_E \mathbf{N}_E^T,$$

where $\mathbf{N}_E$ is the assembling matrix with only zero and one entries.

Clearly, the elemental matrices $\mathbf{A}_E$ must provide accurate quadrature rules for integrals over mesh elements:

$$\int_E \mu_{12} \varepsilon(\mathbf{u}) : \varepsilon(\mathbf{v}) \, \mathrm{d}V = \mathbf{U}_E^T \, \mathbf{A}_E \, \mathbf{V}_E + |E| \, \mathcal{O}(h). \tag{3}$$

To obtain the correct error term, the quadrature rule must be exact iat least for linear velocity functions. To derive such a rule for a general polygon or polyhedron E, we recall first a few facts from linear algebra.

Let $\mathbf{B}_E$ be a full rank $n \times n$ matrix, representing a change of the basis in a linear space. Change of the basis induces the following congruent transformation of the matrix $\mathbf{A}_E$:

$$\hat{\mathbf{A}}_E = \mathbf{B}_E^T \, \mathbf{A}_E \, \mathbf{B}_E.$$

In reality, a partial information about the basis and the matrix $\hat{\mathbf{A}}_E$ is often available. For instance, we know *a priori* how to calculate the integral in (3) for linear functions $\mathbf{u}$, $\mathbf{v}$ and constant tensor μ_{12}. Indeed, in this case, the integrand is a constant. Thus, a natural choice for a basid vector is the vector those components are values of a linear function at vertices of E.

In a more abstract framework, let us assume that we (a) know m basis vectors $\mathbf{B}_i$, $m < n$, and (b) can calculate somehow m vectors $\mathbf{R}_i = \mathbf{A}_E \mathbf{B}_i$ without using the matrix $\mathbf{A}_E$. Then, it is possible to complete the basis in such a way that the matrix $\hat{\mathbf{A}}_E$ is block-diagonal. More precisely, let us complete the basis by vectors $\mathbf{B}_j$, such that

$$\mathbf{B}_j^T \, \mathbf{R}_i = 0, \qquad 1 \le i \le m < j \le n. \tag{4}$$

Then, we have the following identity:

$$\mathbf{B}_E^T \mathbf{A}_E \mathbf{B}_E = \begin{bmatrix} \hat{\mathbf{A}}_E^1 & 0 \\ 0 & \hat{\mathbf{A}}_E^2 \end{bmatrix}.$$

This implies immediately that the (i,k)-entry of matrix $\hat{\mathbf{A}}_E^1$ is the dot-product $\mathbf{B}_i^T \mathbf{R}_k$; therefore, this matrix can be calculated easily.

Detailed analysis reveals that the accuracy requirement (3) alone is not sufficient to build a convergent approximation of the elliptic operator in (2). What is also needed are the orgonality conditions (4).

We define m basis vectors $\mathbf{B}_i$ using the degrees of freedom of linearly independent linear vector-functions $\boldsymbol{\psi}_i$. In 3-D there are twelve such functions, which gives $m = 12$. In 2-D, $m = 6$. Thus, m is always less or equal to the dimension n of matrix $\mathbf{A}_E$ and the equality is achived only for a simplex. Next, we replace the tensor μ_{12} in (3) by a constant tensor μ_E. This is again the order of h approximation. Next, we replace $\mathbf{u}$ by $\boldsymbol{\psi}_i$ and integrate by parts to obtain

$$\begin{aligned} |E|O(h) + \mathbf{B}_i^T \mathbf{A}_E \mathbf{V}_E &= \int_E \mu_E \varepsilon(\boldsymbol{\psi}_i) : \varepsilon(\mathbf{v})\, \mathrm{d}V \\ &= \sum_{f \in \partial E} ((\mu_E \varepsilon(\boldsymbol{\psi}_i)) \cdot \mathbf{n}_E) \cdot \int_f \mathbf{v}\, \mathrm{d}S, \end{aligned} \tag{5}$$

where $\mathbf{n}_E$ is the exterior normal vector to the surface of E. This formula is the remarkable property: for an arbitrary $\mathbf{v}$, the volume integral can be calculated accurately using only the surface information.

For each face f, the surface integral can be calculated approximately using the degrees of freedom at its vertices $\mathbf{v}$. Again, we need only an $O(h)$ approximation. Recall that there exist positive coefficients $\omega_{f,v}$ such that the center of gravity $\mathbf{x}_f$ of face f is a linear combination of vertices $\mathbf{x}_v$ of f:

$$\mathbf{x}_f = \sum_{v \in f} \omega_{f,v} \mathbf{x}_v.$$

These weights give a quadrature rule exact for linear functions. Using them in the formula for $\mathbf{A}_E$ and neglecting the $\mathcal{O}(h)$ terms, we obtain

$$\mathbf{B}_i^T \mathbf{A}_E \mathbf{V}_E = \sum_{f \in \partial E} ((\mu_E\, \varepsilon(\boldsymbol{\psi}_i)) \cdot \mathbf{n}_E) \cdot \sum_{v \in f} \omega_{f,v} \mathbf{V}_{E,v}.$$

After simple re-arranging of the terms, the right-hand side can be written in a compact form as the dot product of two vectors:

$$\sum_{f \in \partial E} ((\mu_E \nabla \boldsymbol{\psi}_i) \cdot \mathbf{n}_E) \cdot \sum_{v \in f} \omega_{f,v} \mathbf{V}_{E,v} = \mathbf{R}_i^T \mathbf{V}_E.$$

Due to arbitrariness of $\mathbf{V}_E$, we derive the desired relations $\mathbf{A}_E \mathbf{B}_i = \mathbf{R}_i$ *without knowledge of the matrix* $\mathbf{A}_E$. Note that our arguments and presented derivations hold for an arbitrarily shaped element.

No information is available to specify the matrix $\hat{\mathbf{A}}_E^2$; thus, it remains arbitrary. For the moment, we use a diagonal matrix, $\hat{\mathbf{A}}_E^2 = \alpha_E \mathbf{I}_E$; however, this freedom can be analyzed in the future. A reasonable choice for the scaling parameter α_E is the mean trace of the first diagonal block, $\alpha_E = \mathrm{trace}(\hat{\mathbf{A}}_E^1)/d$.

To complete the method derivation, we write down the formula for μ_E in element E. For a one-dimensional shock, the 2-D viscousity term reduces to a 1-D model. Therefore, we take the same parameters c_1 and c_2 to obtain

$$\mu_E = \rho_E\, (\gamma + 1)\, L_E \Big(c_1\, s_E - c_2\, L_E\, \widetilde{\varepsilon}_E(\mathbf{U}_E) \Big),$$

where L_E is the characteristic length (preferably in the direction of the shock) and $\widetilde{\varepsilon}_E$ is the negative spectral component of ε_E. The superscript E indicates that a mean value of the related quantatity. According to formula (5), calculation of

the mean value of the symmetrized gradient is reduced to calculation of a surface integral that can be done with the quadrature rule described above.

Numerical experiments

In the experiments shown below, a factor χ_E is added to the μ_E. Note that $\chi_E = 1$ if only if $\text{trace}(\varepsilon_E(\mathbf{U}_E)) < 0$. Otherwise, $\chi_E = 0$. The characteristic length L_E is defined as $|E|^{1/d}$.

Since, our TAV does not control a hourglass distortion of the mesh, additional numerical viscosity is added to the system using the temporal triangular subzoning method [2]. We verified with numerical experiments that both viscosities are required in our simulations.

Let us consider a 3-D Noh implosion problem, where the ideal gas with $\gamma = 5/3$, density $\rho = 1$, and pressure $p = 0$ is given an initial unit inwards radial velocity. A spherical shock wave is generated at the origin and moves with constant speed $1/3$. At time $t = 0.6$, the shock wave has radial coordinate 0.2. The density behind the shock is 64.

First, using symmetry of the problem, we solve it in the r-z geometry. The initial computational mesh is the 80×80 square mesh occupying the unit square. Second, the same problem is solved in three-dimensions. The initial mesh is the $80 \times 80 \times 80$ orthogonal mesh. In both runs $c_1 = 0.5$ and $c_2 = 1.0$. As shown in Fig. 1, the meshes at final time $t = 0.6$ have high-quality elements. The scatter plots in Fig. 2 indicate acceptable preservation of the spherical symmetry. Around the shock, we observe approximately 5% variation of density in the angular direction.

The density behind the shock is smaller than the theoretical value of 64 in both runs. Density oscillations before the shock can be controlled by increasing the coeffcient c_1. Note that the results are more accurate in 3-D.

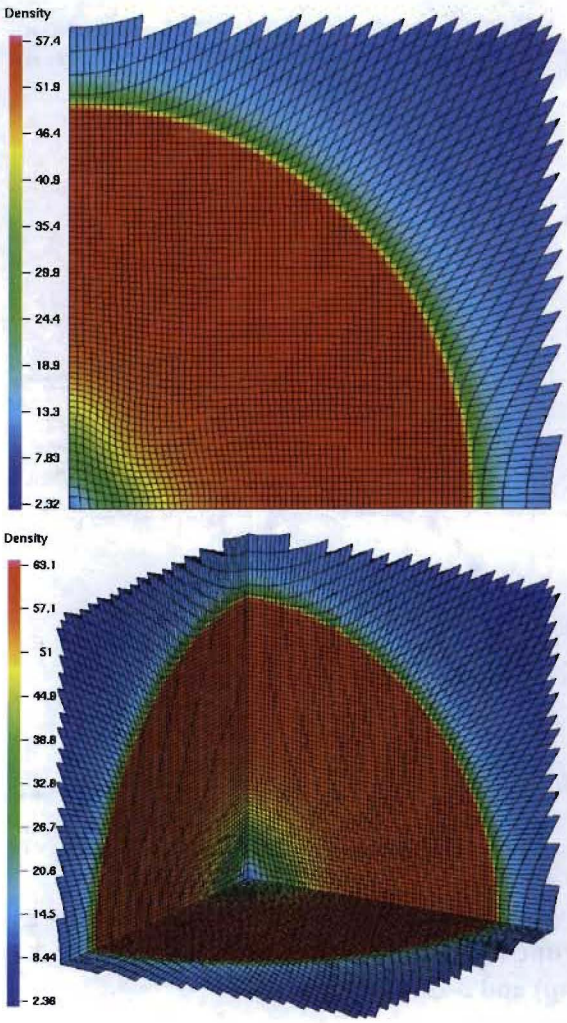

Figure 1: Noh problem: 2-D and 3-D meshes at time t=0.6 colored by the density.

In the second experiment, we consider the Sedov explosion problem. The problem generates a strong diverging shock wave [13, 14]. The initial density of the ideal gas with $\gamma = 1.4$ is unity and the initial velocity is zero. At $t = 0$, the total energy E_0 is all internal and concentrated at the origin. The analytical solution gives the expanding

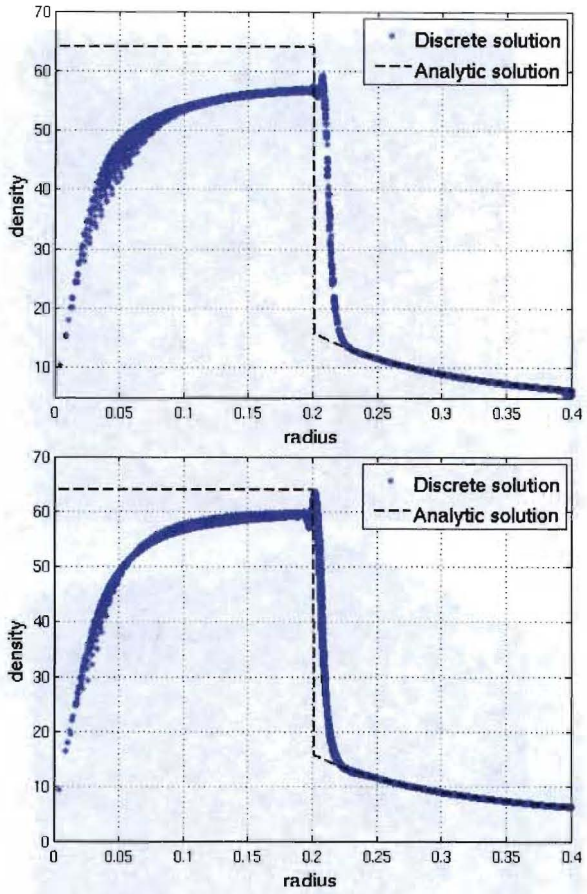

Figure 2: Noh problem: density distribution as a function of the distance from the origin in 2-D (top) and 3-D (bottom) runs.

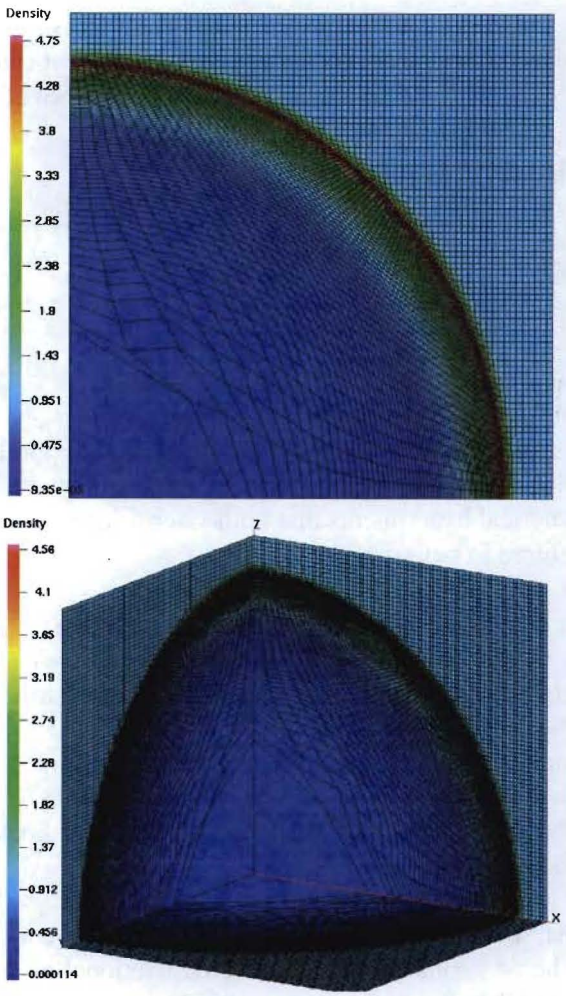

Figure 3: Sedov problem: 2-D and 3-D meshes at time t=1 colored by the density.

shock of radius r_s with peak density of 6,

$$r_s = \left(\frac{E_0 \, t^2}{\alpha_s \, \rho_0} \right)^{0.2},$$

where $\alpha_3 = 0.850937$. The total energy E_0 is defined such that $r_s = 0.9$ at time $t = 1$.

We consider a 80×80 square mesh occupying initially the unit square. Only one element near the origin (the biggest element in Fig. 3) is given a non-zero specific internal energy. The mesh elements are compressed in the radial direction and have large obtuse angles. Note that only small angles (close to 0°) may reduce (theoretically) the accuracy of the mimetic discretization. The pictures in Fig. 4 show small variation of density in the angular direction.

The same problem is solved in three-dimensions. The initial mesh is the $80 \times 80 \times 80$ orthogonal mesh. In both runs $c_1 = c_2 = 1$. The trace of the final mesh at $t = 1$ is shown in Fig. 4. All hexahedra have high quality according to the mesh

criteria formulated in [1] for polyhedral meshes. We recall that presence of large obtuse dihedral angles does not necessary affect the mesh quality. In the bottom picture in Fig. 4, we observe slight reduction of the pike density compared to the two-dimensional simulation (the top-right picture). On the other hand, position of the shock is more accurate in the three-dimensional simulation.

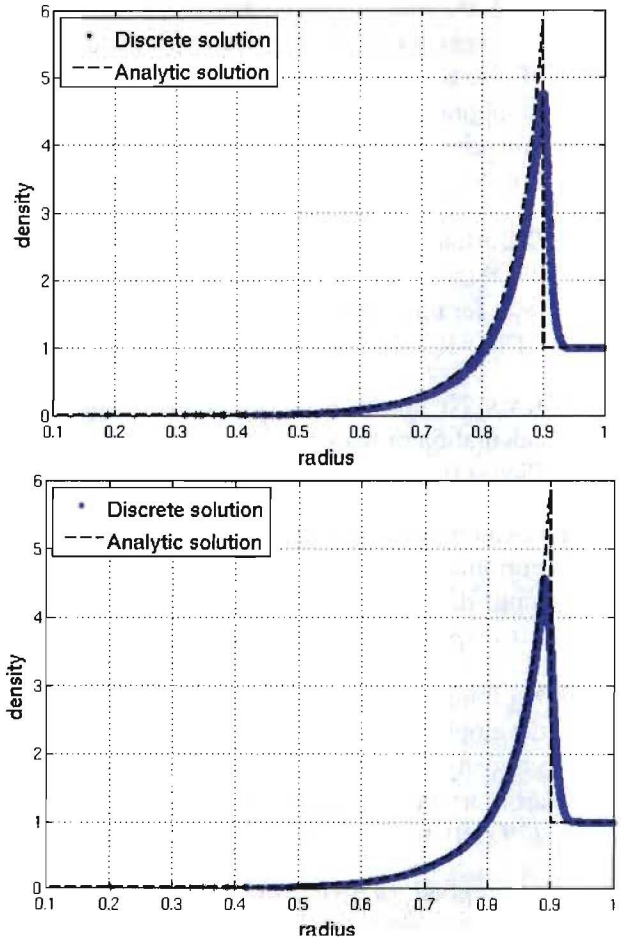

Figure 4: Sedov problem: density distribution as a function of the distance from the origin in 2-D (top) and 3-D (bottom) runs.

In the Saltzman problem, a one-dimensional shock wave propagates through a two-dimensional mesh [11]. This tests the ability of the method to model shock waves that are oblique to the mesh. As artificial viscosity is dominant in the shock wave propagation, the Saltzman piston problem is often used for testing new viscosity methods.

A box is initially filled with the cold ideal gas ($\gamma = 5/3$) at density 1. A piston moves into the box with a constant speed 1.0 and generates a shock wave that reflects from the opposite fixed end of the box at time $t = 0.8$ and hits the piston at time $t = 0.9$. The simulation time is 0.925 when the shock reflected from the piston has not yet reached the fixed end. The final density behind the shock is 20 and the density ahead of the shock is 10.

Figure 5 compares results of simulations in the x-y and r-z coordinate systems. In both runs $c_1 = c_2 = 1$. We observe a slightly more accurate results in the r-z coordinate system. The final mesh lines are more straight in this experiment. A common wall heating effect is observed on the top wall of the box where the symmetry boundary condition is applied.

Conclusion

We constructed a new mimetic tensor artificial viscosity on polygonal and polyhedral meshes. The tensor viscosity is designed as the mimetic discretization of the differential operator $\text{div}\,(\mu\varepsilon(\mathbf{u}))$, where μ is the full second-order tensor coefficient. We demonstrated performance of the new viscosity with three test problems.

Acknowledgements

The simulations were done using the code [3]. We authors acknowledge support of the DOE Office of Science Advanced Scientific Computing Research (ASCR) Program and the Advanced Simulation & Computing (ASC) Program.

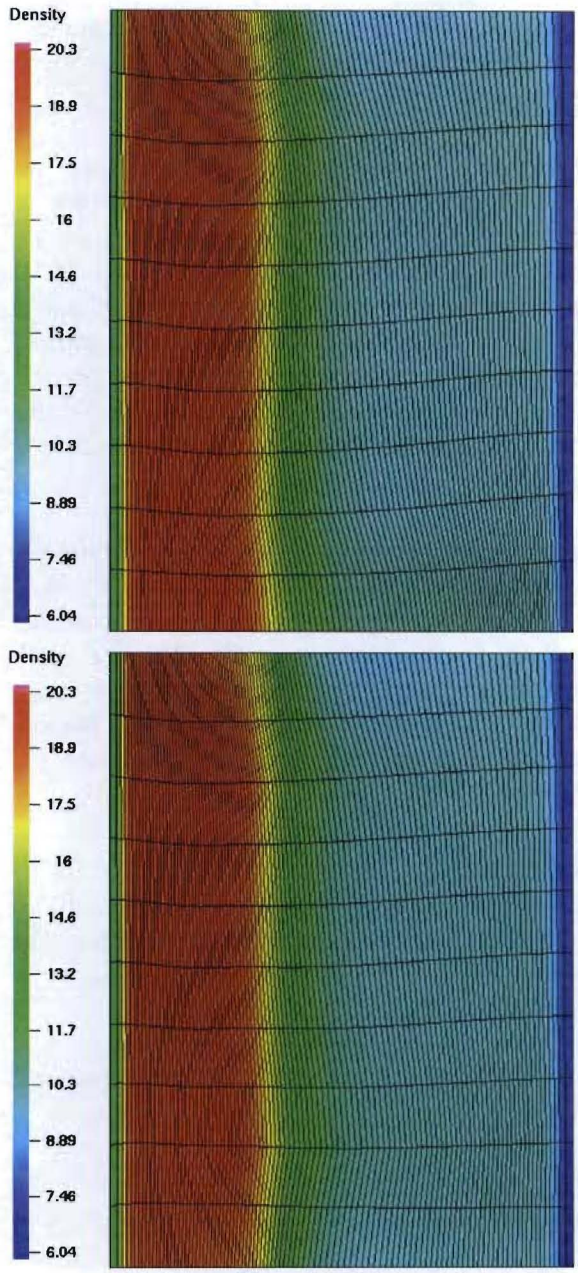

Figure 5: Saltzman problem: meshes at time t=0.925 colored by the density in 2-D simulations using x-y (top) and r-z (bottom) coordinatei systems.

References

[1] F.Brezzi, A.Buffa, K.Lipnikov. Mimetic finite differences for elliptic problems. *M2AN Math. Model. Numer. Anal.* (2009) **43**, 277–295.

[2] P.L. Browne, K.B. Wallick. The reduction of mesh tangling in two-dimensional Lagrangian hydrodynamics codes by the use of viscosity, artificial viscosity, and TTS (temporary triangular subzoning for long, thin zones). Technical Report LA-470-MS, Los Alamos National Laboratory, 1971.

[3] D.Burton. Consistent finite-volume discretization of hydrodynamics conservation laws for unstructured grids. LLNL Report UCRL-JC-118788, 1994.

[4] J. von Neumann, R.Richtmyer. A method for calculation of hydrodynamic shocks. *J. Appl. Phys.* (1950) **21**, 232-237.

[5] E. Caramana, M.Shashkov, P.Whalen. Formulation of artificial viscosity for multi-dimensional shock wave calculations. *J. Comput. Phys.* (1998) **144**, 70–97.

[6] K.Lipnikov, M.Shashkov. A framework for developing a mimetic tensor artificial viscosity for Lagrangian hydrocodes on arbitrary polygonal meshes. *J. Comput. Phys.* **229** (2010), 7911–7941.

[7] J.Campbell, M.Shashkov. A tensor artificial viscosity using a mimetic finite difference algorithm. *J. Comput. Phys.* (2001) **172**, 739–765.

[8] T.Kolev, R.Rieben. A tensor artificial viscosity using a finite element approach. *J. Comput. Phys.* (2009) **228**:22, 8336–8366.

[9] R. Landshoff. A numerical method for treating fluid flow in the presence of shocks.

Technical report LA-1930, Los Alamos National Laboratory, 1955.

[10] W.D. Schulz. Tensor artificial viscosity for numerical hydrodynamics. *J. Math. Phys.* (1964) **5**, 133-138.

[11] J. Saltzman, P. Colella. Second order corner coupled upwind transport methods for Lagrangian hydrodynamics. Technical Report LA-UR-85-678, Los Alamos National Laboratory, 1985

[12] A.A. Samarskii, Yu.P. Popov. Difference methods for gasdynamics, Nauka, Moscow, 1992, in Russian.

[13] L. Sedov. *Similarity and Dimensional methods in mechanics*. Academic Press, New York, 1959.

[14] A. Shestakov. Time-dependent simulations of point explosion with heat conduction. *Physics of Fluids* (1999), **11**, 1091–1095.

[15] M. Wilkins. Use of artificial viscosity in multidimensional shock wave problems. *J. Comput. Phys.* (1980) **36**, 281–303.